Hindawi Publishing Corporation
International Journal of Photoenergy
Volume 2012, Article ID 832516, 7 pages
doi:10.1155/2012/832516

Research Article

Investigation on the Photoelectrocatalytic Activity of Well-Aligned TiO_2 Nanotube Arrays

Xiaomeng Wu,[1,2] Zhaohui Huang,[1] Yangai Liu,[1] and Minghao Fang[1]

[1] *School of Materials Science and Technology, China University of Geosciences-Beijing, Beijing 100083, China*
[2] *School of Materials Science and Engineering, Beijing University of Aeronautics and Astronautics, Beijing 100191, China*

Correspondence should be addressed to Zhaohui Huang, huang118@cugb.edu.cn

Received 29 August 2011; Revised 5 November 2011; Accepted 5 November 2011

Academic Editor: Jiaguo Yu

Well-aligned TiO_2 nanotube arrays were fabricated by anodizing Ti foil in viscous F^- containing organic electrolytes, and the crystal structure and morphology of the TiO_2 nanotube array were characterized and analyzed by XRD, SEM, and TEM, respectively. The photocatalytic activity of the TiO_2 nanotube arrays was evaluated in the photocatalytic (PC) and photoelectrocatalytic (PEC) degradation of methylene blue (MB) dye in different supporting solutions. The excellent performance of ca. 97% for color removal was reached after 90 min in the PEC process compared to that of PC process which indicates that a certain external potential bias favors the promotion of the electrode reaction rate on TiO_2 nanotube array when it is under illumination. In addition, it is found that PEC process conducted in supporting solutions with low pH and containing Cl^- is also beneficial to accelerate the degradation rate of MB.

1. Introduction

Photocatalysis of the TiO_2 semiconductor has received increasing attention for the application of degrading a great variety of organic contaminants in water, and the interest lies in the simplicity and low cost of the photocatalytic system which is mainly composed of an ultraviolet or a visible light source and the TiO_2 [1–9]. Up to now, improving the photocatalytic efficiency of TiO_2 thin-film photoreactors remains a major task in achieving maximum potential in commercial applications. Fortunately, this task can be fulfilled to a great extent by (1) using nanoporous TiO_2 films to increase the active surface area for photoreactions; (2) applying a positive potential bias on TiO_2 photocatalysts to suppress markedly the recombination rate of photogenerated electrons and holes. Under potential bias conditions, the photocatalytic reactions on TiO_2 surface may be considered as special electrode reactions involving electron-hole (e-h) pairs on TiO_2 photoelectrode/liquid interface. Inspired by the concept of achieving charge separation in a semiconductor system with an electrochemical bias introduced by Fujishima and Honda [10], an externally applied anodic bias is induced to the field of photocatalysis to improve the degradation efficiency and received satisfying results [11–14].

A new form of photocatalyst, TiO_2 nanotube arrays possessing higher quantum efficiency, less grain boundaries, and more excellent adsorption ability derives from its specific structure than compact or nanoporous films comprised of randomly oriented nanoparticles, has demonstrated its potential in environmental applications and exhibited a remarkably improved photocatalytic activity as compared to traditional films [15–22]. However, few studies have been intentionally reported dealing with the possibility to use in situ photoelectrogenerated active chlorine to improve pollutants degradation rate [23, 24]. Therefore, in this study, we have examined the effects of applied potentials, electrolyte, and pH value on the photoelectrocatalytic (PEC) degradation of MB over TiO_2 nanotube array, and the effect of in situ generated active chlorine during the PEC degradation of MB was also evaluated. The motivation of this work is to gain an insight into the photoelectrocatalytic degradation characteristics of organic matters by TiO_2 nanotube arrays, and to offer fundamental information for the practical application of PEC in wastewater treatment.

2. Experimental

2.1. Synthesis of TiO_2 Nanotube Arrays. TiO_2 nanotube arrays were synthesized by anodic oxidation of titanium foil (0.1 mm thick, 99.6% purity). The titanium foil surface was treated before oxidation as follows: degrease in acetone, etch in mixed acid of HF and HNO_3 (concentrated solution, volume ratio 1 : 9), and rinsed with deionized water followed by drying in a cold air stream. The anodic oxidation was carried out in a two-electrode cell, with a platinum plate as the counter electrode. The electrochemical treatment consisted of potential ramping from the open-circuit potential to the target potential and then being held for a specified time period. The electrolyte was NH_4F (0.5 wt %) in mixed solvent of glycol and deionized water with a volume ratio of 9 : 1; the oxidation potential and period were 50 V and 0.5 h. After anodic oxidation, the samples were rinsed in deionized water and dried in a cold air stream. A subsequent thermal annealing of the oxide layer was carried out at 500°C in N_2 for 1 h using a heating rate of 10°C/min and cooling naturally in order to convert the amorphous oxide into anatase phase.

2.2. Characterization of Photocatalysts. X-ray diffraction (XRD, Bruker D8 Advance) was used to examine the crystal structure of the nanocomposites. The morphologies of the samples were examined by field emission scanning electron microscopy (FESEM, Hitachi S-4800), and transmission electron microscope (TEM, JEOL 2010F) was used for investigating the microstructure of the samples. Photoelectrochemical measurements were performed with an IM6ex Potentiostat.

2.3. Photoelectrocatalytic Activity Tests. All the electrochemical measurements were carried out with a universal electrochemical interface and an impedance spectrum analyzer Zahner IM6e. The instrument was connected with a conventional three-electrode system (TiO_2 nanotube array with effective electrode area of 1 cm^2, a saturated calomel electrode (SCE) and a Pt foil served as the working electrode, reference electrode, and counter electrode, resp.) which was established on a quartz beaker containing 600 mL test solution. For the experiments of PC and PEC oxidation, the TiO_2 nanotube array electrode (4 cm^2) were used as the photoanode, while a Pt electrode and a saturated calomel electrode (SCE) were used as counter and reference electrodes, respectively. All voltages reported are versus SCE unless otherwise noted. About 100 mL of 10 mg L^{-1} aqueous MB solution was served as target pollutant, in which 0.1 M NaCl and 0.1 M Na_2SO_4 was added as supporting electrolyte, respectively. The solution pH value was adjusted by adding a small quantity of HCl, H_2SO_4, or NaOH. Both the PC and PEC oxidation reactions were carried out in a certain photoreactor system, and 250 W metal-halogen lamp (CMH-2500) with intensity of 100 mW/cm^2 was used as simulated solar light and the visible wavelength was controlled through a 400 nm cut filter. The MB concentrations were measured using UV-2100 spectrophotometer (SHIMADZU, Japan).

3. Results and Discussion

3.1. Characterization of TiO_2 Nanotube Array. Figure 1 shows FESEM images of TiO_2 nanotube arrays formed by anodization. It is clear that TiO_2 layer consists of nanotube arrays with a uniform tube diameter of 100 nm, a wall thickness of 25 nm, and the thickness of the layer is approximately 2.6 μm. It is also apparent that pore mouths are open on the top of the layer while on the bottom of the structure the tubes are closed. As shown in Figure 1(c), the magnified top-view image of the TiO_2 nanotube array after annealing indicates the TiO_2 layer retained its structural integrity. Figure 2 shows XRD patterns of the TiO_2 nanotube array before and after annealing in N_2 at 500°C for 1 h. It is apparent that as-anodized TiO_2 shows only the peaks from a Ti substrate, while the annealed sample shows clearly the crystalline signature of anatase, in other words the as-anodized TiO_2 exhibits an amorphous structure.

3.2. Photoelectrochemical Characterization of TiO_2 Nanotube Array. The photoelectrochemical current density reflects the generation, separation, and transfer efficiency of photoexcited electrons from the valence to the conduction band of TiO_2. Photocurrent-potential curves under dark conditions (curve I) and under illumination, both in 0.1 mol L^{-1} Na_2SO_4 (curve II) and NaCl (curve III) are compared to each other in Figure 3. According to the literature [25], by illuminating the semiconductor with light energy greater than that of the band gap, electron-hole pairs are generated at the electrode surface. A bias potential positive to the flat-band potential produces a bending of the conduction band causing a more effective charge separation and increases the photocurrent (i_{ph}) that begins to flow and likely promotes a better oxidative degradation process. As expected, Figure 4 shows that, under illumination, TiO_2 photoelectrode gives rise to a photocurrent in Na_2SO_4 at −0.20 V, but in NaCl media the onset potential shifts to a less positive potential of −0.38 V, both at pH = 6.0. In addition to this shift in potential, photocurrent in NaCl media was also higher than in Na_2SO_4 electrolyte.

In comparing curves II and III in Figure 3, one can notice that the nature of the electrolyte could affect the photocurrent intensity. The photocurrent intensity obtained for sulphate solutions corresponds simply to the contribution from the injection of electrons in the conduction band and hole transfer rate scavenged by OH^-. On the other hand, it is assumed that chloride ions might be oxidized at a less positive potential under photoelectrocatalytic conditions compared to that of electrochemical conditions as denoted by the following [24, 26]:

$$TiO_2\text{-}h_{vb}{}^+ + Cl_s{}^- \longrightarrow TiO_2\text{-}Cl_s{}^\bullet \quad (1)$$

$$2Cl_s{}^\bullet \longrightarrow Cl_2 \quad (2)$$

$$Cl_2 + H_2O \longrightarrow Cl^- + HClO + H^+ \quad (3)$$

The dependence of photocurrent and dye discoloration rate on chloride concentration may be attributed to the

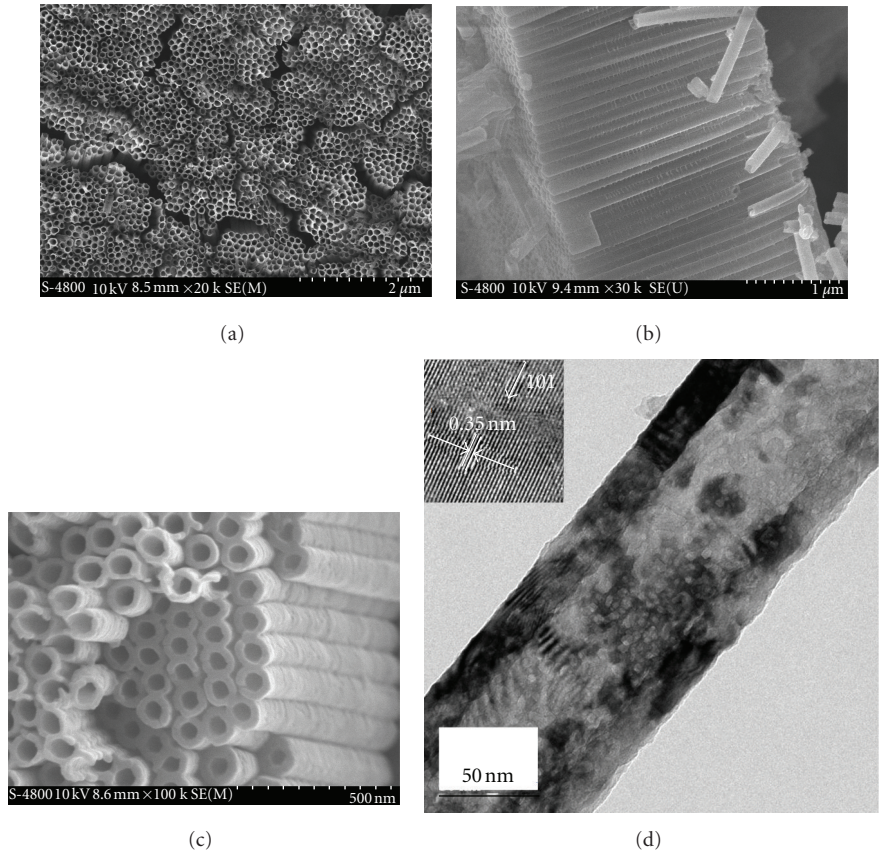

Figure 1: FESEM top-view images (a) and cross-section (b) of TiO_2 nanotube arrays and the magnified image of the TiO_2 nanotube arrays after annealing (c). TEM images of a typical annealed single TiO_2 nanotube (d) and high magnification image showing a lattice spacing of 0.35 nm, corresponding to anatase phase (inset).

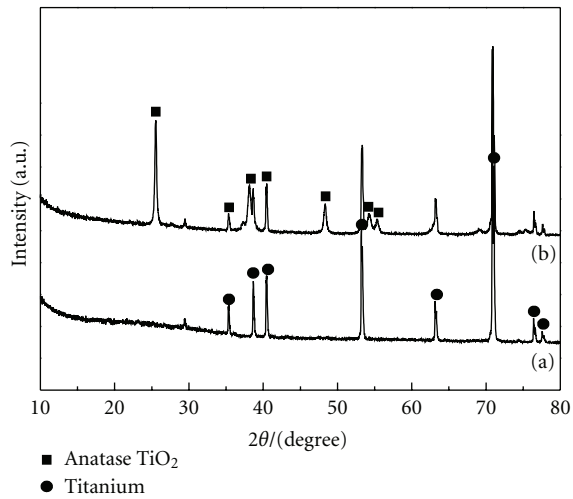

Figure 2: XRD patterns of as-prepared TiO_2 nanotube arrays before and after annealing in N_2 stream at 500°C for 1 h.

improvement of Cl^- adsorption on the electrode surface under conditions of high concentrations of chloride [19]. At higher adsorption conditions, electron/holes generated at a steady rate or $OH^\bullet$ radicals are more easily transferred to the Cl^- ions improving the photocatalysis process due to the minimization of charge recombination.

Besides, the small visible light response, as shown in the inset of Figure 3, may indicate a slight modification of TiO_2 bandgap derived from carbon incorporation in our experiment. Considering the TiO_2 nanotube array was prepared in organic electrolytes, it is assumed that organic residue (glycol) might provide carbon source to react with the TiO_2 matrix to form $TiO_{2-x}C_x$ at high temperature under inert atmosphere [27], and the EDX analysis demonstrated that the sample which contained a small fraction of carbon remains (2.79 wt%) after annealing. The bandgap reduction extends the utilization of solar energy to visible light region while the intragap band introduction allows the absorption of visible photons of even lower energy and the carbon-doping enables the TiO_2 nanotubes to absorb longer wavelength light which is further verified by UV-Vis spectra shown in Figure 4. The strength of photoresponse depends on the density of states in the bands, and the increase of carbon-doping density in the TiO_2 thin films increases the density of states of the valence band edge and the intragap band, thereby enhancing the photoresponse of TiO_2 nanotubes [28]. However, the reactivity of the holes generated in the intragap band toward oxidation of MB is assumed to be low because the density of states in the

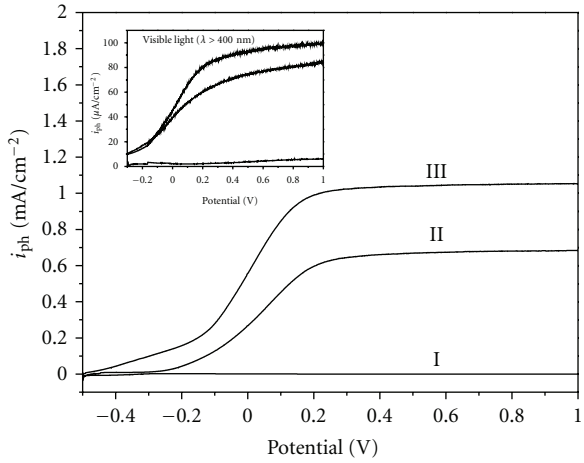

Figure 3: Photocurrent-potential curves obtained for TiO_2 nanotube arrays electrode under dark conditions (curve I) and for 0.1 mol L^{-1} Na_2SO_4 (curve II) and 0.1 mol L^{-1} NaCl (curve III) under illumination (complete solar spectrum). The inset shows the corresponding visible light response of the electrode ($\lambda > 400$ nm). Scan rate = 10 mV s^{-1}, pH = 6.0.

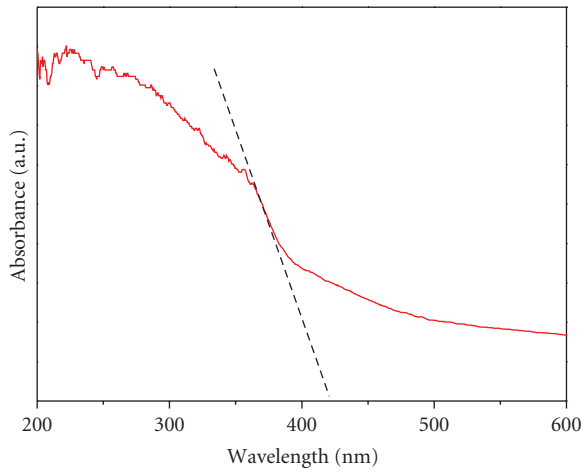

Figure 4: UV-Vis diffuse reflectance spectrum (DRS) for TiO_2 nanotube array.

intragap band is much smaller than that in the valence and conduction bands [29].

The evaluation of the stability of the above TiO_2 nanotube arrays is carried out by potentiostatic (current versus time, *I-t*) measurements. Figure 5 shows the *I-t* curve obtained from the PEC cell containing Pt as the cathode and TiO_2 (4 cm^2) as a photoanode. It shows about 1.0 mA/cm^2 current density when an external bias of +0.6 V electrode is applied to the TiO_2 nanotubes electrode. The photocurrent value goes down to zero as soon as the illumination of light on the photoanode is stopped, and the cell is run intermittently for 25 min without sacrificing the photocurrent. This result suggests that the photogenerated charge carriers transfer effectively from the working electrode to the counter electrode and the great activity of TiO_2 nanotube array in the photocatalysis process.

3.3. Comparison of Rate Constants for PC or PEC Processes. The UV spectra of MB in the PEC process (biased at +0.6 V) at various reaction intervals are presented in Figure 6. The reduction in absorbance is likely due to the degradation of the MB chromophore, and the peak shift is due to demethylation occurring both at the catalyst surface and bulk solution [30]. It is well documented that the MB degradation meets the first-order photoelectrocatalytic reaction rate and its kinetics can also be expressed as $\ln(C/C_0) = kt$, where k is the apparent rate constant, t is the illumination time, and C and C_0 are the actual reaction and initial concentration of MB solution, respectively. Figure 7 shows the degradation kinetic curves as a function of time recorded for the TiO_2 nanotube array by PC and PEC, respectively. In the case of PEC, applied potentials ranged between 0 and +0.6 V and absorbance decay at 664 nm was monitored over 15 min of the experiment, an almost completed degradation (96.74%) was observed around 90 min at a low bias level of +0.6 V, while the MB degradation ratio for PC process only achieves to 26.32% and reaction rate constant is 0.00297 min^{-1}. It is evident that the degradation efficiency of PEC is considerably higher than that of PC at the same time and it increases with the applied potential bias; the corresponding reaction rate constants are 0.00933 min^{-1}, 0.02298 min^{-1}, 0.03501 min^{-1}, 0.04747 min^{-1} for external bias potential at 0 V, 0.2 V, 0.4 V, and 0.6 V, respectively. These results clearly demonstrate that the degradation rate increases as a function of applied potential up to $E = +0.6$ V. It was reported that further increases in potential lead to a slight reduction in degradation. The reason should be attributed mainly to the evolution of the oxygen bubbles at the surface of the TiO_2 nanotubes which hinders electrode reaction.

As calculated from onset potential measurements (Figure 3), the flat-band potential for TiO_2 at pH = 6.0 in 0.1 mol L^{-1} NaCl media is about 0.38 V. All of the applied potentials employed in this study are positive of this flat-band potential. Therefore, there is always a potential gradient over the TiO_2 film, resulting in an electric field, which keeps photogenerated charges apart. Since the magnitude of the limiting current is a measure of the overall photoelectrocatalytic performance of an electrode, theoretically, the degradation rate of PEC should reach its maximum when the photocurrent is in saturation; however, the overall MB degradation efficiency still maintains an increasing trend despite the photocurrent being almost constant when the bias potential is higher than +0.2 V, as seen in Figure 3, and the plausible explanation of the phenomenon may be ascribed to that more positive potential bias favors the specific adsorption of Cl^- on the surface of TiO_2 nanotube array electrode; therefore in situ photoelectrochemically generated active chlorine that can diffuse into bulk solution to react with MB, differing from $OH^\bullet$ radicals that usually only survive in the region of interface is responsible for the further enhancement of degradation rate of MB with increasing positive bias potential.

3.4. Effect of Supporting Electrolyte. The supporting electrolyte also plays an important role in a photoelectrocatalytic process, and the effect of the supporting electrolyte on the

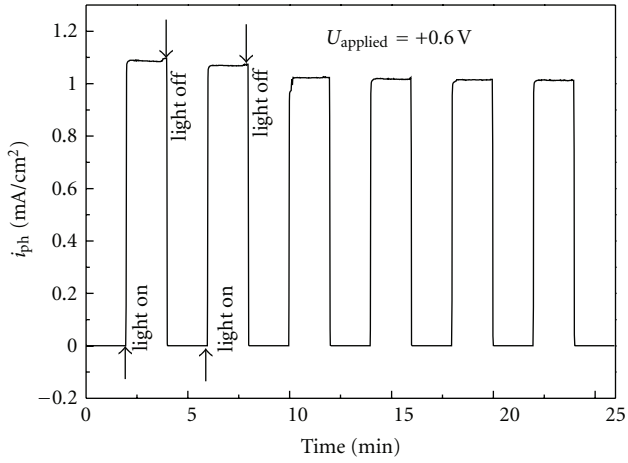

FIGURE 5: Photocurrent densities versus time of TiO_2 nanotubes array being applied with 0.6 V bias potential (versus SCE) under simulated solar light illumination. A 0.1 M NaCl solution was used as the electrolyte.

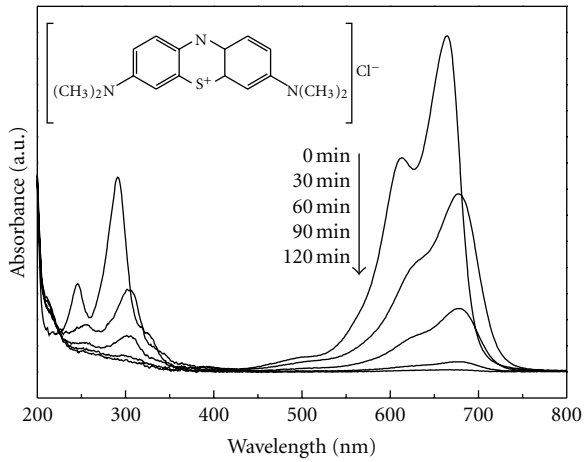

FIGURE 6: Change of UV-Vis spectra of methylene blue at various reaction intervals for PEC process in the presence of +0.6 V versus SCE anodic bias. Inset is the chemical structure of MB.

performance of TiO_2 nanotubular arrays was tested monitoring the degradation of 10 mg L^{-1} of MB in 0.1 mol L^{-1} of Na_2SO_4 and NaCl. Figure 8 shows the influence of the type of electrolyte on the removal of color investigated through experiments conducted with 10 mg L^{-1} MB in 0.1 mol/L NaCl and 0.1 mol/L Na_2SO_4, respectively. The higher degradation rate is observed in chloride media, indicating that the mechanism of MB degradation in NaCl solution is different than that operating in the other non-chloride containing supporting electrolytes. Obviously, the result is in line with the photocurrent difference between curves II and III in Figure 3; one can notice that the nature of the electrolyte affects the photocurrent response. It seems that the photocurrent intensity obtained for sulphate solutions corresponds simply to the contribution from the injection of electrons in the conduction band and hole transfer rate scavenged by OH^- [31]. Nevertheless, it is

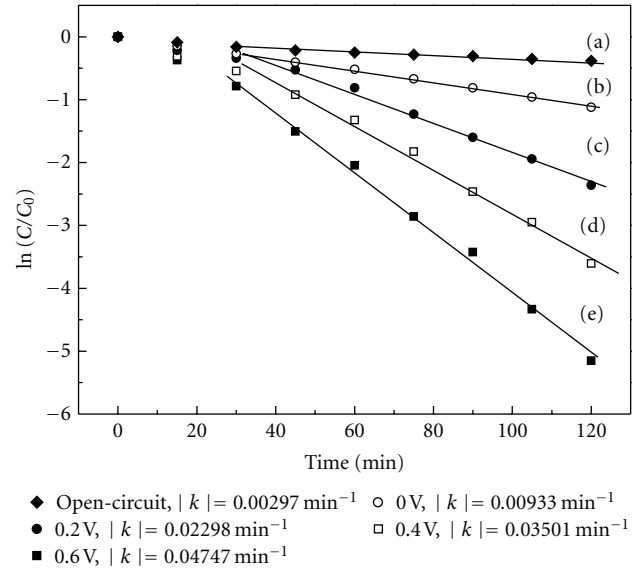

FIGURE 7: MB degradation kinetic curves of TiO_2 nanotube array under various conditions.

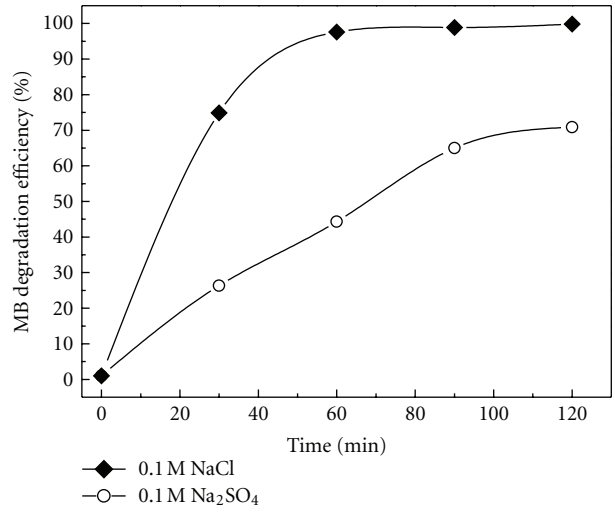

FIGURE 8: The comparison of degradation efficiency via PEC route in 0.1 M NaCl and Na_2SO_4, bias at 0.6 V.

known that chloride ions are commonly electrochemically oxidized to chlorine at potentials over +1 V, and as stated above, chloride ions could be oxidized to form some active chloride species at a less positive potential under photoelectrocatalytic conditions which was confirmed by the more detailed studies of Hepel and Hazelton [32]. Therefore, the comparing experiment illustrates that the selection of suitable supporting electrolyte also favors the improvement of degradation efficiency in photoelectrocatalytic system.

3.5. Effect of Solution pH Value. The influence of pH on the discoloration rate of MB is presented in Figure 9. Initial degradation rates are plotted as function of different pH values (C_0 = 10 mg L^{-1}, E = +0.6 V, and 0.1 mol L^{-1} NaCl).

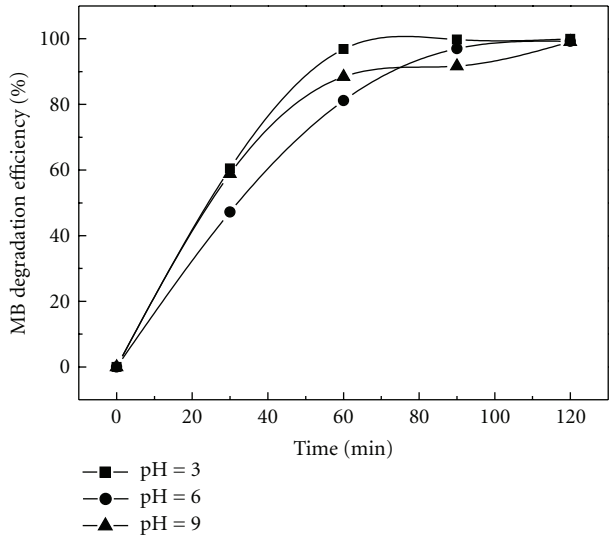

Figure 9: Effect of solution pH on photoelectrocatalytic degradation of MB.

It can be seen that the degradation rate is highest over the pH range 4~6 and decreases noticeably at higher pH. These results show that color removal is to a great extent faster at acidic medium but mineralization could be preponderant at pH $\geqslant$ 6. In all further investigations pH = 6.0 was selected as the optimum pH to investigate the dye degradation using chlorine medium, where mineralization and color removal are favorable. Since TiO_2 usually has an isoelectric point at a pH 5.7, it would seem that at pH values higher than the isoelectric point, negative ions (e.g., Cl^-) are repelled from the TiO_2 surface leading to lower degradation efficiencies. As a consequence, both the percentage of chlorine generation and the adsorption of the dye are diminished in conditions where the pH of the solution is higher than the pH of isoelectric point [33]. In alkaline solutions, the formation of $OH^\bullet$ radicals is predominant over $Cl^\bullet$ radicals and Cl_2 but the kinetics of MB degradation is still slower than in acidic media. In addition, it should be noted that the noticeable change of the degradation efficiency at pH = 9 during the PEC process is considered to be due to the constantly decreased concentrations of the OH^-, which is responsible for hydroxyl radical generation and the degradation of the MB during the photocatalytic oxidation process [34].

4. Conclusion

The photocatalytic degradation efficiency of methylene blue (MB) in aqueous solutions showed a remarkable increase by means of illumination with electroassisted way in the presence of TiO_2 nanotube array electrode. The rate constant of photoelectrocatalytic degradation was greater than that of photocatalytic processes either in isolation or as a sum of individual processes, indicating an obviously synergistic effect among photo- and electroprocesses. In addition, low pH and high concentration of Cl^- solutions are beneficial to the degradation rate of MB. In situ photoelectrocatalytic generated active chlorine that can diffuse into the bulk solution should be responsible for the enhancement of degradation rate of MB. Hence, the photoelectrocatalytic process with in situ generated active chlorine will be an attractive method in the treatment of wastewater.

Acknowledgments

The authors gratefully acknowledge the financial support to this work from the National Natural Science Foundation of China (no. 51032007) and the New Star Technology Plan of Beijing (no. 2007A080).

References

[1] M. Grandcolas, A. Louvet, N. Keller, and V. Keller, "Layer-by-layer deposited titanate-based nanotubes for solar photocatalytic removal of chemical warfare agents from textiles," *Angewandte Chemie - International Edition*, vol. 48, no. 1, pp. 161–164, 2009.

[2] T. L. Thompson and J. T. Yates, "Surface science studies of the photoactivation of TiO_2—new photochemical processes," *Chemical Reviews*, vol. 106, no. 10, pp. 4428–4453, 2006.

[3] M. Radecka, M. Rekas, E. Kusior et al., "TiO_2-based nanopowders and thin films for photocatalytical applications," *Journal of Nanoscience and Nanotechnology*, vol. 10, no. 2, pp. 1032–1042, 2010.

[4] R. Asahi, T. Morikawa, T. Ohwaki, K. Aoki, and Y. Taga, "Visible-light photocatalysis in nitrogen-doped titanium oxides," *Science*, vol. 293, no. 5528, pp. 269–271, 2001.

[5] D. V. Bavykin, J. M. Friedrich, and F. C. Walsh, "Protonated titanates and TiO_2 nanostructured materials: synthesis, properties, and applications," *Advanced Materials*, vol. 18, no. 21, pp. 2807–2824, 2006.

[6] Y. Z. Fan, G. P. Chen, D. M. Li et al., "Highly selective deethylation of rhodamine B on TiO_2 prepared in supercritical fluids," *International Journal of Photoenergy*, vol. 2012, Article ID 173865, 7 pages, 2012.

[7] S. Wang, L. Zhao, J. Ran, Z. Shu, G. Dai, and P. Zhai, "Effects of calcination temperatures on photocatalytic activity of ordered titanate nanoribbon/SnO_2 films fabricated during an EPD process," *International Journal of Photoenergy*, vol. 2012, Article ID 472958, 7 pages, 2012.

[8] S.-J. Kim, N.-H. Lee, H.-J. Oh, S.-C. Jung, W.-J. Lee, and D.-H. Kim, "Photocatalytic properties of nanotubular-shaped TiO_2 powders with anatase phase obtained from titanate nanotube powder through various thermal treatments," *International Journal of Photoenergy*, vol. 2011, Article ID 327821, 7 pages, 2011.

[9] J. A. Byrne, P. A. Fernandez-Ibañez, P. S.M. Dunlop, D. M.A. Alrousan, and J. W.J. Hamilton, "Photocatalytic enhancement for solar disinfection of water: a review," *International Journal of Photoenergy*, vol. 2011, Article ID 798051, 12 pages, 2011.

[10] A. Fujishima and K. Honda, "Electrochemical photolysis of water at a semiconductor electrode," *Nature*, vol. 238, no. 5358, pp. 37–38, 1972.

[11] N. Chandrasekharan and P. Y. Kamat, "Improving the photoelectrochemical performance of nanostructured TiO_2 films by adsorption of gold nanoparticles," *Journal of Physical Chemistry B*, vol. 104, no. 46, pp. 10851–10857, 2000.

[12] X. Z. Li, H. L. Liu, P. T. Yue, and Y. P. Sun, "Photoelectrocatalytic oxidation of rose Bengal in aqueous solution

using a Ti/TiO_2 mesh electrode," *Environmental Science and Technology*, vol. 34, no. 20, pp. 4401–4406, 2000.

[13] M. C. Li and J. N. Shen, "Photoelectrochemical oxidation behavior of organic substances on TiO_2 thin-film electrodes," *Journal of Solid State Electrochemistry*, vol. 10, no. 12, pp. 980–986, 2006.

[14] J. Li, L. Zheng, L. Li, Y. Xian, and L. Jin, "Fabrication of TiO_2/Ti electrode by laser-assisted anodic oxidation and its application on photoelectrocatalytic degradation of methylene blue," *Journal of Hazardous Materials*, vol. 139, no. 1, pp. 72–78, 2007.

[15] Y. Lai, L. Sun, Y. Chen, H. Zhuang, C. Lin, and J. W. Chin, "Effects of the structure of TiO_2 nanotube array on Ti substrate on its photocatalytic activity," *Journal of the Electrochemical Society*, vol. 153, no. 7, pp. D123–D127, 2006.

[16] Y. Lai, H. Zhuang, L. Sun, Z. Chen, and C. Lin, "Self-organized TiO_2 nanotubes in mixed organic-inorganic electrolytes and their photoelectrochemical performance," *Electrochimica Acta*, vol. 54, no. 26, pp. 6536–6542, 2009.

[17] D. Wang, T. Hu, L. Hu et al., "Microstructured arrays of TiO_2 nanotubes for improved photo-electrocatalysis and mechanical stabili," *Advanced Functional Materials*, vol. 19, no. 12, pp. 1930–1938, 2009.

[18] S. P. Albu, A. Ghicov, J. M. Macak, R. Hahn, and P. Schmuki, "Self-organized, free-standing TiO_2 nanotube membrane for flow-through photocatalytic applications," *Nano Letters*, vol. 7, no. 5, pp. 1286–1289, 2007.

[19] G. Zhang, H. Huang, Y. Zhang, H. L. W. Chan, and L. Zhou, "Highly ordered nanoporous TiO_2 and its photocatalytic properties," *Electrochemistry Communications*, vol. 9, no. 12, pp. 2854–2858, 2007.

[20] Z. Xu and J. Yu, "Visible-light-induced photoelectrochemical behaviors of Fe-modified TiO_2 nanotube arrays," *Nanoscale*, vol. 3, no. 8, pp. 3138–3144, 2011.

[21] J. Yu and B. Wang, "Effect of calcination temperature on morphology and photoelectrochemical properties of anodized titanium dioxide nanotube arrays," *Applied Catalysis B*, vol. 94, no. 3-4, pp. 295–302, 2010.

[22] J. Yu, G. Dai, and B. Cheng, "Effect of crystallization methods on morphology and photocatalytic activity of anodized TiO_2 nanotube array films," *Journal of Physical Chemistry C*, vol. 114, no. 45, pp. 19378–19385, 2010.

[23] J. S. Do and W. C. Yeh, "In situ degradation of formaldehyde with electrogenerated hypochlorite ion," *Journal of Applied Electrochemistry*, vol. 25, no. 5, pp. 483–489, 1995.

[24] M. V. B. Zanoni, J. J. Sene, and M. A. Anderson, "Photoelectrocatalytic degradation of Remazol Brilliant Orange 3R on titanium dioxide thin-film electrodes," *Journal of Photochemistry and Photobiology A*, vol. 157, no. 1, pp. 55–63, 2003.

[25] M. Radecka, M. Rekas, A. Trenczek-Zajac, and K. Zakrzewska, "Importance of the band gap energy and flat band potential for application of modified TiO_2 photoanodes in water photolysis," *Journal of Power Sources*, vol. 181, no. 1, pp. 46–55, 2008.

[26] X. F. Cheng, W. H. Leng, O. Y. Pi, Z. Zhang, J. Q. Zhang, and C. N. Cao, "Enhancement of photocatalytic activity of TiO_2 film electrode by in situ photoelectro-generating active chlorine," *Transactions of Nonferrous Metals Society of China (English Edition)*, vol. 17, no. 5, pp. 1087–1092, 2007.

[27] S. Liu, L. Yang, S. Xu, S. Luo, and Q. Cai, "Photocatalytic activities of C-N-doped TiO_2 nanotube array/carbon nanorod composite," *Electrochemistry Communications*, vol. 11, no. 9, pp. 1748–1751, 2009.

[28] W. H. Leng, Z. Zhang, J. Q. Zhang, and C. N. Cao, "Investigation of the kinetics of a TiO_2 photoelectrocatalytic reaction involving charge transfer and recombination through surface states by electrochemical impedance spectroscopy," *Journal of Physical Chemistry B*, vol. 109, no. 31, pp. 15008–15023, 2005.

[29] C. Xu and S. U. M. Khan, "Photoresponse of visible light active carbon-modified -n-TiO_2 thin films," *Electrochemical and Solid-State Letters*, vol. 10, no. 3, pp. B56–B59, 2007.

[30] L. Rizzo, J. Koch, V. Belgiorno, and M. A. Anderson, "Removal of methylene blue in a photocatalytic reactor using polymethylmethacrylate supported TiO_2 nanofilm," *Desalination*, vol. 211, no. 1–3, pp. 1–9, 2007.

[31] M. F. Brugnera, K. Rajeshwar, J. C. Cardoso, and M. V. B. Zanoni, "Bisphenol A removal from wastewater using self-organized TiO_2 nanotubular array electrodes," *Chemosphere*, vol. 78, no. 5, pp. 569–575, 2010.

[32] M. Hepel and S. Hazelton, "Photoelectrocatalytic degradation of diazo dyes on nanostructured WO_3 electrodes," *Electrochimica Acta*, vol. 50, no. 25-26, pp. 5278–5291, 2005.

[33] J. Luo and M. Hepel, "Photoelectrochemical degradation of naphthol blue black diazo dye on WO_3 film electrode," *Electrochimica Acta*, vol. 46, no. 19, pp. 2913–2922, 2001.

[34] M. Hepel and J. Luo, "Photoelectrochemical mineralization of textile diazo dye pollutants using nanocrystalline WO_3 electrodes," *Electrochimica Acta*, vol. 47, no. 5, pp. 729–740, 2001.